

# We are IntechOpen, the world's leading publisher of Open Access books Built by scientists, for scientists

6,900

Open access books available

185,000

International authors and editors

200M

Downloads

Our authors are among the

154

Countries delivered to

TOP 1%

most cited scientists

12.2%

Contributors from top 500 universities



WEB OF SCIENCE™

Selection of our books indexed in the Book Citation Index  
in Web of Science™ Core Collection (BKCI)

Interested in publishing with us?  
Contact [book.department@intechopen.com](mailto:book.department@intechopen.com)

Numbers displayed above are based on latest data collected.  
For more information visit [www.intechopen.com](http://www.intechopen.com)



# The Development of Eddy Current Technique for WWER Steam Generators Inspection

Valentin Uchanin and Vladimir Najda

*Karpenko Physico-Mechanical Institute of National Academy of Sciences,  
Paton Electric Welding Institute, design bureau,  
Ukraine*

## 1. Introduction

Safety and efficiency of nuclear power plants (NPP) are dependent of the technical state of heat exchanger tubes installed in steam generators (SG). The majority of Russian and Ukrainian WWER type NPP units as well as NPP in Czech Republic (Temelin) and Bulgaria (Kozloduy) are equipped by PGV-1000 type SG. These NPP units were introduced into service from 1982 to 2004. Decommissioning dates (or dates of life time prolongation) are planned from 2012 to 2034 (Balitskii et al., 2005). SG heat exchanger tubes create a barrier between the radioactive primary and secondary water circuits and are one of the most critical component in NPP due different type defects and damages initiated during in-service life (Neklyudov et al., 2006; Mytrofanov et al., 2008). The in-service defects appear along the full tube length and in the zone of the tubes mounting to collector desk. Therefore, the complex diagnostics of heat exchanger tubes based on the trustworthy results of nondestructive testing is the question of great importance (IAEA-TECDOC-981, 1997; IAEA-EBP-VVER-11, 1998; IAEA-TECDOC-1400, 2004).

## 2. State of the art

The routine examinations of SG tubes along the full length are executed by eddy current (EC) method which has many advantages in comparison with methods based on other physical phenomena. Different type internal EC probes for SG tubes inspection are developed. The most known are bobbin, rotational and array EC probe (Alferink & Meier, 1996; Amedro et al., 1983; Werner et al., 1987; Clark, 1993; Cecco et al., 1996; Herka et al., 1999; Krajcovic & Plasek, 2006). Each type of EC probe has advantages and limitations shortly analyzed in Table 1. At the present time the largest amount of SG tube inspections are executed by the internal bobbin type probes application. The main reasons of such choice are high inspection speed, lowest price, large flaw detection experience and established tradition. Particularly, the bobbin type EC probes are only one type of probes applied at Ukrainian NPP for full length tube inspection (Mytrofanov et al., 2008; Uchanin, 2009).

For inspection data interpretation many theoretical and experimental investigations were carried out (Ida, 1986; Pichenot et al., 2004). In another investigations special algorithms, based on feature extraction, neural network, etc, were proposed (Wong et al., 1995; Song et al., 2003; Sabbagh et al., 2008; Nam et al., 2009). But the mentioned results were obtained

mostly for SG tubes of another types then used at WWER type NPP. Thus for appreciable understanding of the results obtained during PGV-1000 type SG tube inspection the subsequent signal response investigation are steel needed. And reliable detection and the quantification of defects is still difficult task.

Next actual question of EC probe application is the passing ability across full tube length. This problem is especially significant for SG tubes of WWER type NPP because of considerable tube geometry disturbances and clogging by deposits.

	Advantages	Disadvantages
Bobbin probe	1) High sensitivity to axial cracks. 2) High inspection speed. 3) Determination of defect location in axial direction. 4) Determining defect depth and length. 5) High reliability and durability. 6) Comparatively low price.	1) Low sensitivity to circumferential cracks. 2) Unrecognizing and false interpretation when several defects are situated with the same axial location.
Rotating probe	1) High sensitivity to cracks of different orientation. 2) Crack orientation determination. 3) Length and depth of crack determination. 4) Determination of defect location in axial direction. 5) Good inspection results visualization.	1) Low inspection speed. 2) Comparatively low reliability and durability. 3) Comparatively low passing ability. 4) High price.
Array probe	1) High sensitivity to cracks of different orientation. 2) High inspection speed. 3) Crack orientation determination. 4) Determination of flaw location in axial direction. 5) Determination of defect parameter.	1) Very high price. 2) Comparatively low reliability and durability. 3) Comparatively low passing ability.

Table 1. Comparative analysis of different type EC probe features.

The next key component important for SG reliability and life-time growth is considered to be the junction points in which tubes are mounted to the collector wall (Balitskii et al., 2005). PGV-1000 SG operating experience shows that the collector material is exposed to stress corrosion, which leads to stress corrosion cracking of collector wall between tube holes (Melechov & Pochmurskij, 2003). Thus, the task is to detect cracks in the collector wall, which are developed mainly from the tube holes. For detection of this crack through tube wall it is possible to use more complicated low frequency EC technique. For such inspection only totally automatic inspection due the influence of radioactive environment can be offered.

SG tubes have 16.0 mm in diameter with 1.5 mm wall thickness and are fabricated of nonmagnetic stainless steel 08X18N10T (AISI 321). The collector wall is fabricated of low-

alloy pearlitic ferromagnetic steel 10GN2MFA with a wall thickness of 171 mm. The inner surface of collectors is plated by 07H25N13 steel cladding. The tube ends are flared in the collector wall and welded to the cladding steel layer. There are 119 vertical and 110 horizontal rows of tube inlet holes accessible from the inner surface of the collector. Thus, the total number of inlet holes is more than 11000. The placement of inlet holes from the collector side and some dimensions are shown in Fig. 1.

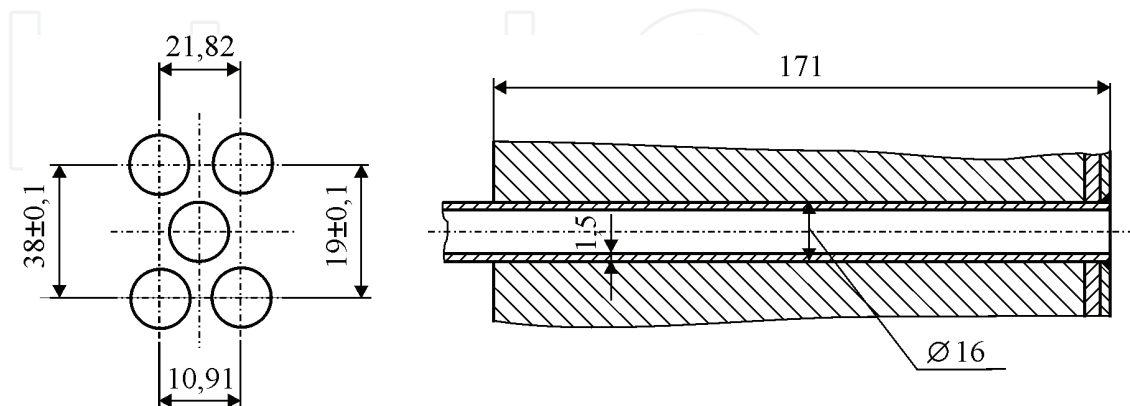


Fig. 1. The scheme of inlet holes placement on the inner surface of collector (left) and heat exchanger tube mounted in collector wall (right).

### 3. The investigation and development of eddy current bobbin probes for SG heat exchanger tubes inspection

#### 3.1 Model based eddy current bobbin probe defect signal response analysis

A differential type bobbin EC probe consists of two opposite connected identical coils. Because of such connection differential bobbin probes are insensitive to gradual changes of tube wall thickness and temperature. Due this feature differential bobbin EC probes are used for defect detection only. The computational model (Fig. 2) deals with a differential bobbin EC probe placed in a tube of stainless 08X18N10T steel, which corresponds to the heat exchanger SG tubes. The 08X18N10T steel specific conductivity was specified to be 1.2 MSm/m. The geometric parameters of the investigated EC probe (internal  $r_1$  and external  $r_2$  radii, length  $l_0$ , the number of turns  $w$ , and the base of placement of the windings  $l_b$ ) can be changed in process of calculations, and, hence, we succeed in optimizing their choice for a specific object and inspection conditions. The defect is located in the tube so that its midpoint corresponds to  $X$  coordinate zero point. The EC probe signal responses were determined by the volume integral method application (Dunbar, 1985; Sabbagh et al, 2008). There were calculated the changes in the real  $X_D$  and imaginary  $R_D$  components of the EC probe impedance  $Z_D$  as well as signal response amplitude  $Mod Z_D$  at operational frequency 100 kHz in the course of EC probe scanning along the tube (the  $X$  coordinate was varied by 1 mm within the range  $\pm 10$  mm) from cracks of different length  $l_{cr}$ , located symmetrically with respect to the  $X$  coordinate zero point (Fig. 2). The computations were performed for the differential EC probe in which internal  $r_1$ , external  $r_2$  radii and winding length  $l_0$  equal to 4.7; 5.1 and 1.6 mm respectively. The number of turns of the coil windings is  $w = 60$ . The inductance of each coil winding in the absence of tested object is equal to 5.5  $\mu$ H, which corresponds with the measured inductance of a real EC probe with the same parameters. The differentially connected coils are separated with distance  $l_b = 3.0$  mm. The crack depth

remained unchanged and was taken equal to 0.5 mm, and crack width (opening) was 0.2 mm. To reach high calculation accuracy, we chose the number of cells in the crack volume over width, length and depth equal to 8, 32 and 16 cells respectively (Uchanin, 2009).

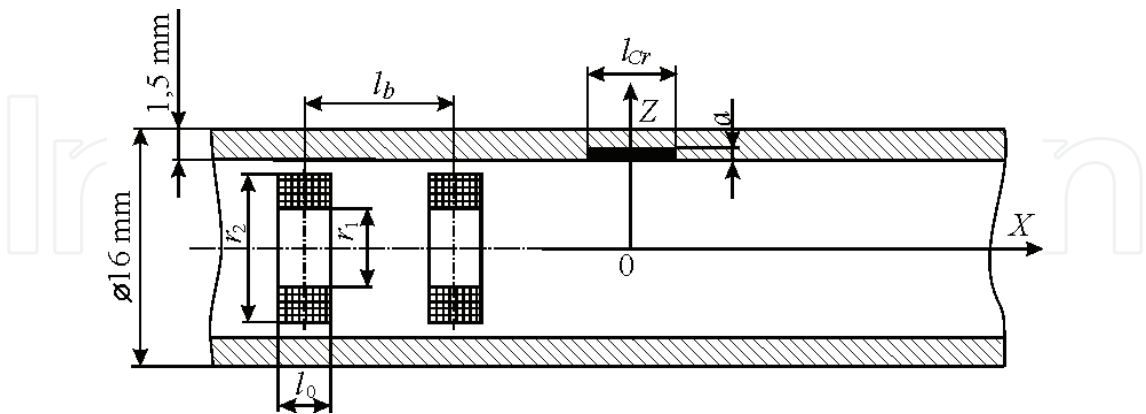


Fig. 2. The dimensions and relative position of the bobbin type EC probe and crack in the tested heat exchanger tube.

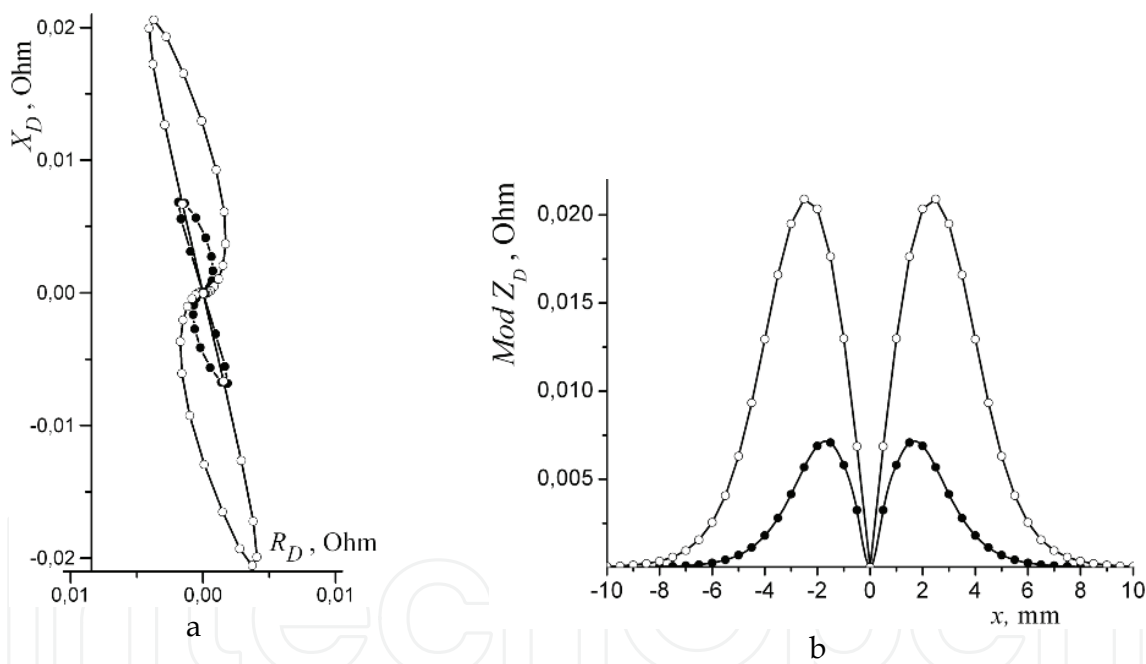


Fig. 3. EC probe signal response scanning hodographs (a) and amplitude distributions (b) for transverse (●) and longitudinal (○) cracks with length  $l_{cr} = 5.0$  mm.

It was established (Fig. 3) that the scanning hodographs and distributions of the EC probe signal amplitude for longitudinal and transverse cracks are similar. The EC probe signal response obtained from a longitudinal crack is approximately thrice as larger against the signal response for transverse crack of the same size. It was noticed that the EC probe begins to “sense” a transverse crack at a distance of 5–6 mm from its center and a longitudinal crack at 7–8 mm. If the EC probe is located symmetrically with respect to the defect the signals responses of separated coil are equal and the output EC probe signal response is equal to zero, which was expected for the differential connection of windings. In addition, it is

necessary to notice that for internal surface (with respect to the EC probe) crack, the imaginary component of the signal response at the operational frequency 100 kHz is four to five times greater than the real component.

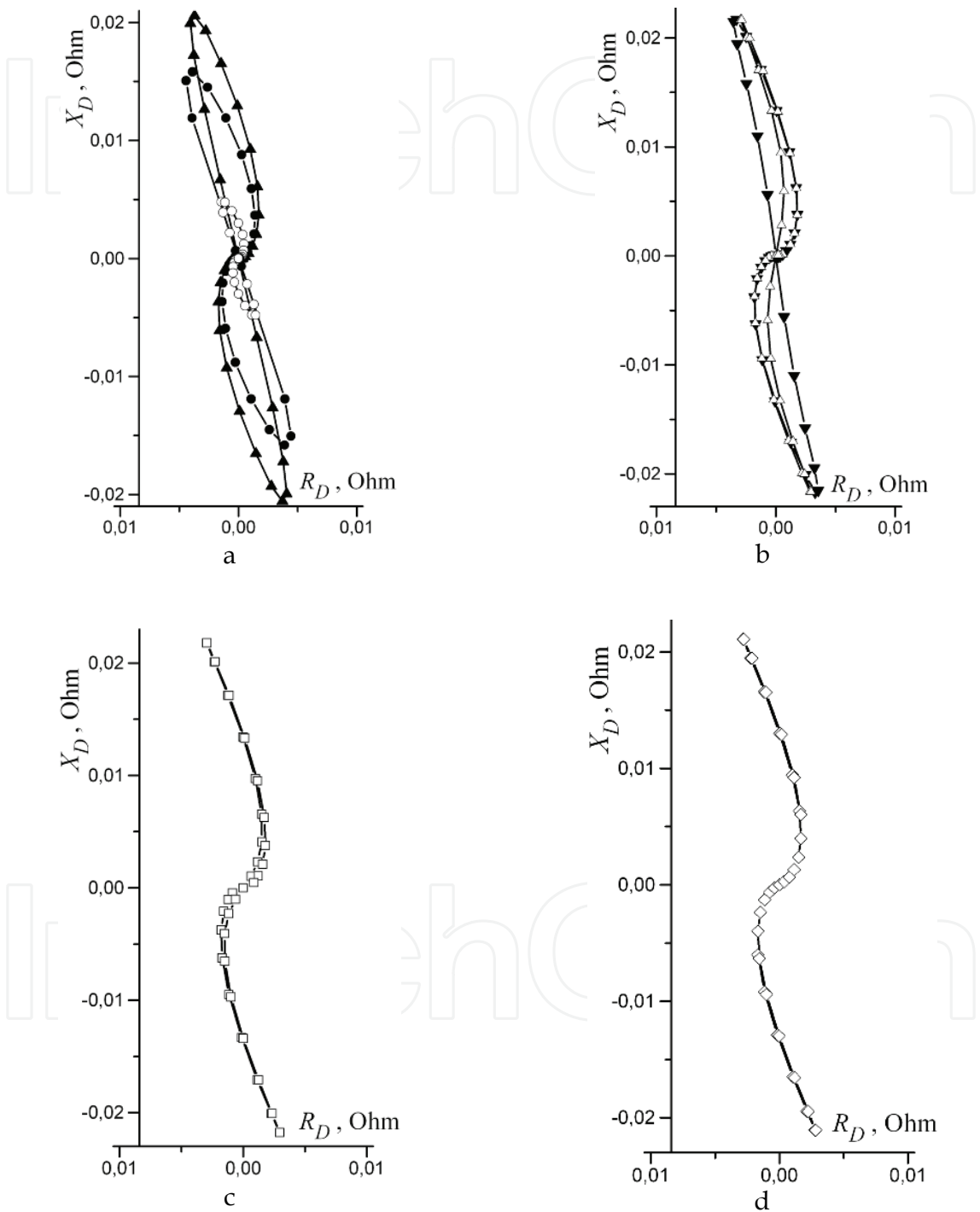


Fig. 4. EC probe signal response scanning hodographs for longitudinal cracks of different length  $l_{cr}$  : a - 1.0 (○), 3.0 (●) and 5.0 mm (▲); b - 6.0 (▼) and 8.0 mm (Δ); c - 10.0 mm (□); d - 12.0 mm (◇).

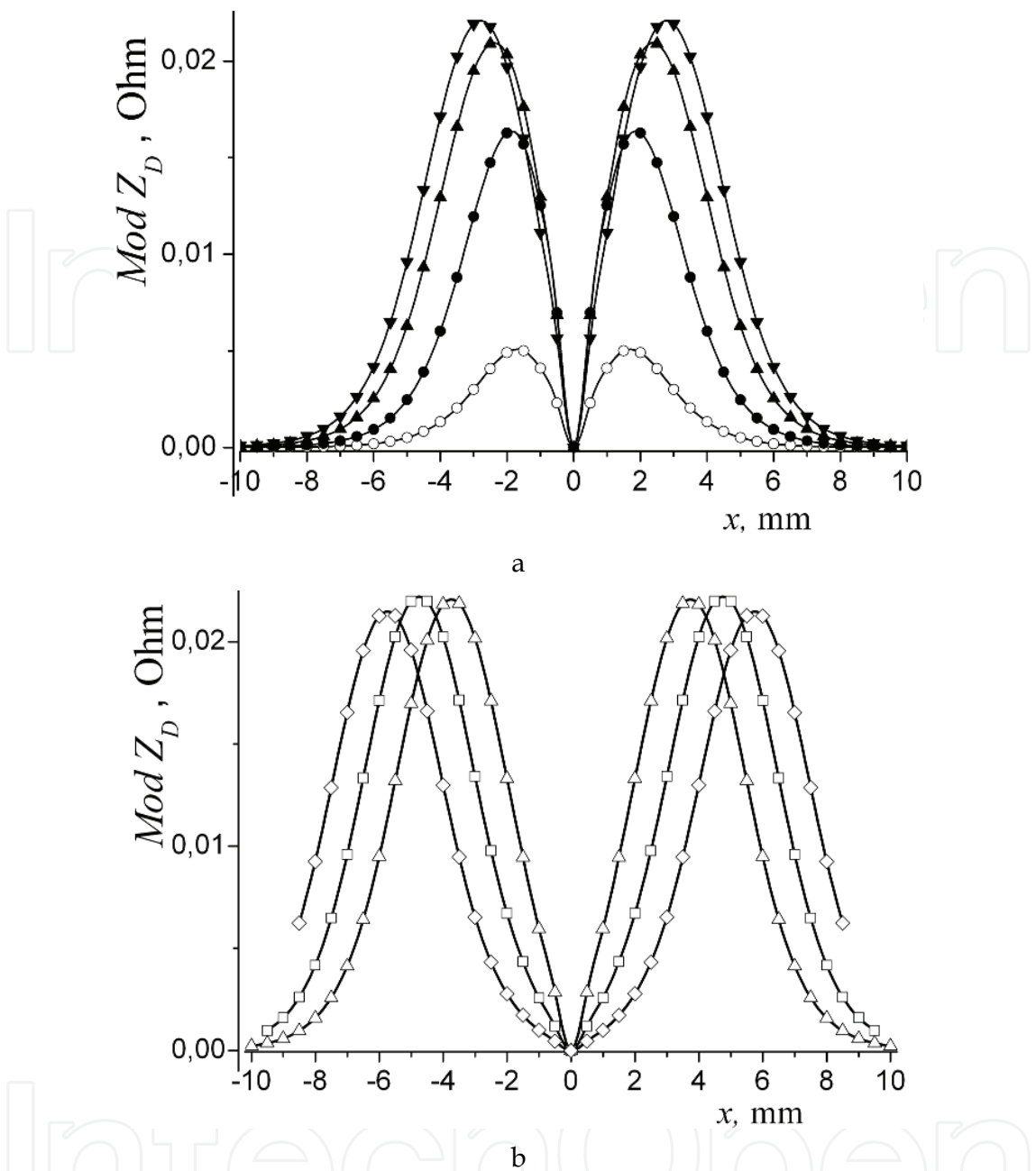


Fig. 5. Signal response amplitude distributions for longitudinal cracks of different length  $l_{cr}$  : a – 1.0 (○), 3.0 (●), 5.0 (▲) and 6.0 mm (▼); b – 8.0 (Δ), 10.0 (□) and 12.0 mm (◇).

The signal response hodographs (Fig. 4) have a characteristic ansiform shape, which is well known from experimental investigations (Alferink & Meier, 1996). It is possible to observe here certain differences for cracks of different length. The hodographs of short cracks ( $l_{cr} < 5$  mm, Fig. 4a) have a figure-of-eight shape with characteristic rounded part, which begins from the zero point, when the EC probe does not sense the crack yet, and continue to the point of maximum signal response amplitude, and nearly linear part, which connects the points of maximum signal amplitude. In the linear part, the signal response amplitude changes most significantly per unit of change in the X coordinate and this is reflected in a greater distance between these points. For a crack length  $l_{cr} = 6$  mm (Fig. 4b), the linear part



of hodograph begins to bend and with further increase in the length come nearer towards its rounded part (Fig. 4c). For long cracks ( $l_{cr} > 10$  mm), the parts of increase and decrease in the signal amplitude and the corresponding points on hodographs are coincided. (Fig. 4d). These features of the EC probe signal response formation for cracks of different length have a physical interpretation and can be explained by the simultaneous influence of the beginning and the end of a crack on the EC probe coils for short cracks. For some values of the defect length, the phenomena indicated above are confirmed in some investigations (Pichenot et al., 2004; Bisiaux et al., 2006).

It was established (Fig. 4 and 5) that the signal response amplitude from a longitudinal crack depends on its length for cracks not longer than 6 mm. We observe here inessential changes in the signal phase, which are manifested in a slight turn of the hodograph in the complex plane. Under the subsequent crack length increase the amplitude and slope of hodograph of EC probe signal response remain practically invariable. Note that, for short longitudinal (1 mm) and transverse cracks, the coordinates of maxima correspond to the base  $l_b = 3.0$  mm of the coil windings placement. The amplitude distribution of EC probe signal response for cracks of length more 1 mm depends on their length (Fig. 5). Hence, knowing the signal distribution, we can determine crack lengths. It should be noted that, in determining the length of long cracks from the Z coordinates, where the signal amplitude is greater than the threshold of operation of the flaw detector, we can obtain a significant error whose sign and value depend on the assigned threshold of sensitivity. More exact results can be obtained if, for this purpose, the coordinates of maximum values of the amplitude distributions of signals will be used. From Fig. 6 we can see that the distance  $l_{Max}$  between coordinates of maximum amplitude correlate with crack length  $l_{cr}$  very good. Insignificant data scattering can be explained by discrete choice of crack length in calculations.

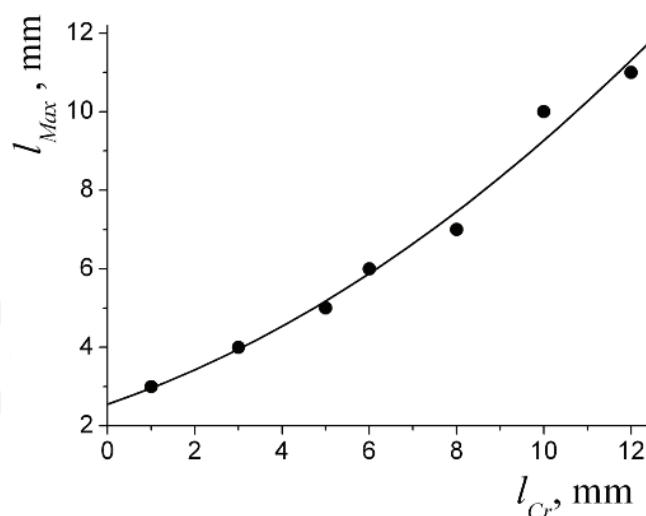


Fig. 6. Influence the crack length  $l_{cr}$  on the distance  $l_{Max}$  between maxima points of longitudinal cracks signal response distribution.

So, we have studied the distribution of the signal responses of internal bobbin EC probes for cracks of different orientation and length in the SG heat exchangers tubes. Some specific features of hodographs and signal amplitudes for cracks of different length were established. The results obtained can be used for the interpretation of the EC probe signal responses and adjustment of the inspection procedures.



The result of inspection must contain not only the information about the presence of defect, though it is also very important. The main task is to predict the subsequent operating time without tube leakage, when defect during its growth reach the opposite surface of tube, independently of internal or outer tube surface was damaged from the beginning. Such estimation can be carried out, when the parameters of detected defects will be evaluated with the fracture mechanic approaches. Such parameter as “metal loss” or defect volume very often is applied in practice (Neklyudov et al., 2006). But for small opening fatigue crack the tube damage and safety are not accompanied by loss of material. To our opinion the residual tube thickness is the better operability criterion to make decision about tube plugging. It is clear, the residual thickness can be obtained from the defect depth measurement results independently of the tube surface the defect was initiated. Therefore the defect depth and residual thickness very often are estimated in percent of tube thickness. The defect width and length also influence the tube durability and availability, but don't have priority importance for estimation of leakage possibility.

To analyze the problems in inspection results interpretation the signal response amplitude and phase in dependence of defect parameters were investigated. In contrast to previous investigations, when the signal response distribution was calculated, the dependence of signal response parameters in specified points defined during the scanning along the tested tube (for example in the point of maximum signal amplitude) must be the main point of interest. That is why, for next calculations the absolute type EC probe it is convenient to apply, because the signal response maximum for defect will be correspond the zero point of X coordinate ( $x = 0$  in Fig. 2). Hereupon the probe winding parameters were selected the same as in previous calculations.

The changes of the EC probe signal response amplitude  $Mod Z_D$  and phase  $\varphi$  at operational frequency 100 kHz for longitudinal cracks on internal tube surface, when probe is situated in zero point ( $x = 0$ ), in dependence of depth  $a$ , width (opening)  $c$  and length  $l_{cr}$  were defined (Fig. 7-9). The signal response amplitudes were balanced and normalized in respect to signal response of EC probe situated in defect-free zone of tube.

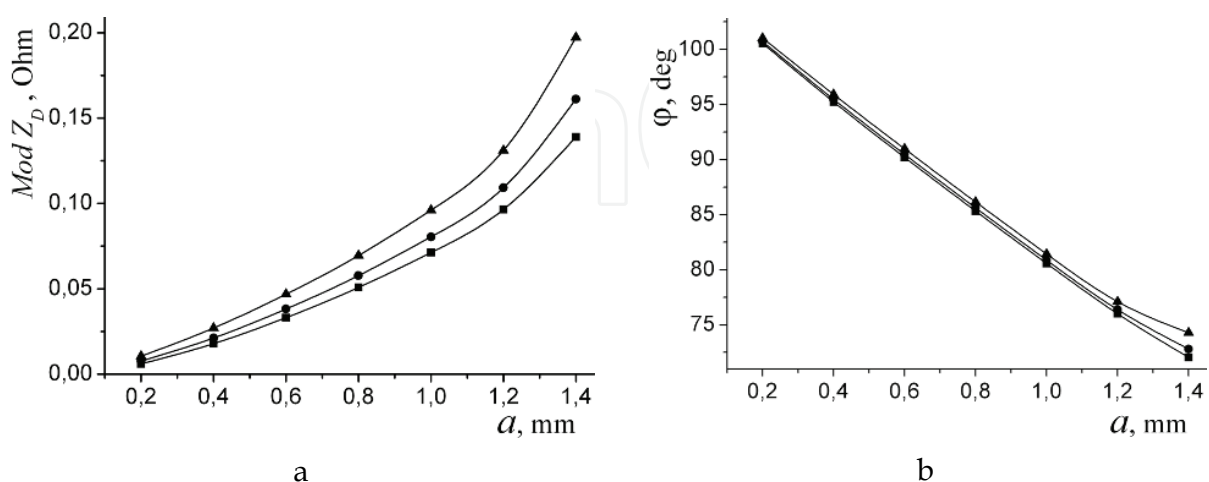


Fig. 7. Influence of crack depth  $a$  on the amplitude  $Mod Z_D$  (a) and phase  $\varphi$  (b) for longitudinal 6 mm long crack with width 0.1 mm (■); 0.2 mm (●) and 0.4 mm (▲).

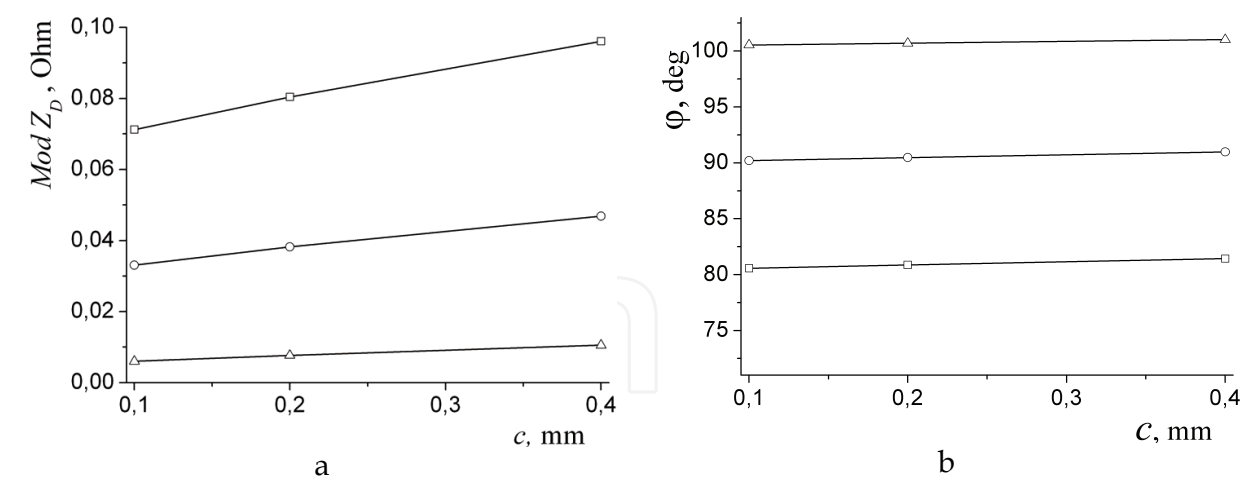


Fig. 8. Influence of crack width  $c$  on the amplitude  $Mod Z_D$  (a) and phase  $\varphi$  (b) for longitudinal 6.0 mm long crack with depth 0.2 mm ( $\Delta$ ); 0.6 mm ( $\circ$ ) and 1.0 mm ( $\square$ ).

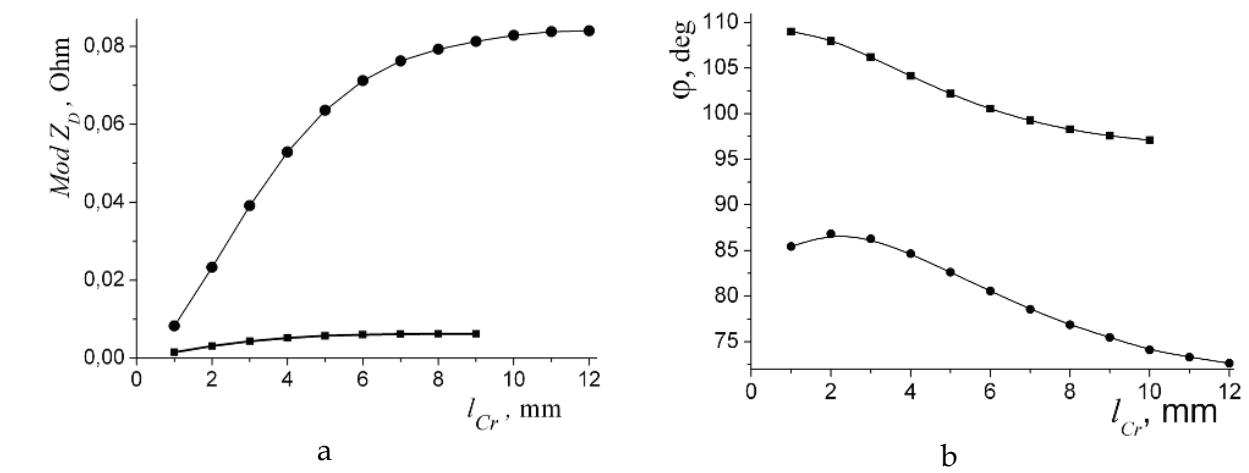


Fig. 9. Influence of crack length  $l_{cr}$  on the amplitude  $Mod Z_D$  (a) and phase  $\varphi$  (b) for longitudinal crack with depth 0.2 mm ( $\blacksquare$ ) and 1.0 mm ( $\bullet$ ).

Presented results show strong amplitude-depth and phase-depth EC probe defect signal response dependence. In our case, the amplitude is increased more than to one order and phase is changed more than 30 degrees, when crack depth is changed from 0.2 mm to 1.4 mm. The dependence of signal response amplitude becomes stronger with the crack depth growth. It is especially noticed, when crack depth is more than 1.2 mm, what is fitted with experimental results (Alferink & Meier, 1996). The amplitude-depth dependence (Fig. 7a) coincides with experimental results obtained for artificial electro-erosion defects and introduced stress corrosion cracks in tubes identical to our calculation mode (Krajcovic & Plasek, 2006).

As we can see on Fig. 7b the phase-depth curves for cracks with different width are very close each other to draw a conclusion about the invariant property of phase relatively the crack width changes. This conclusion is confirmed by dependences on Fig. 8b, where it was shown that crack depth weakly influence the signal response phase. As it was mentioned before, similar conclusion it is impossible to say about the signal response amplitude.

It is necessary to emphasize, that the phase is not the invariant parameter relatively the crack length, when the crack depth it is needed to be defined, especially for short cracks. Such influence of crack length to signal response phase is low in comparison with the crack depth influence. At least, two defects with 0.2 mm and 1.4 mm depths can be differentiated by phase measurements even for high difference in crack length (Fig. 9b). More accurate algorithm for crack length estimation can be established from the signal response distribution (see Fig. 5) (Uchanin, 2009). In this case, for crack depth estimation it is possible to use the phase-depth dependences obtained for previously defined crack length.

Let us consider the signal response features for local defects with different depths originated from internal and outer tube surfaces. Calculations were carried out for absolute type EC probe (with only one winding) moved along X axis (Fig. 2). It was considered local corrosion (like pitting) defect simulated by 1 mm diameter circular hole with flat bottom. Depths of holes were increased from 0.3 mm to through wall condition, when 1.5 mm depth was reached. As in previous calculations, EC probe signals were balanced relatively EC probe signal for unflawed tube. Operational frequency was 100 kHz as in previous investigations. On next figures the EC probe signal response scanning hodographs in complex plane for different depth holes situated on internal (fig. 10a) and external (fig. 10b) tube surfaces were plotted.

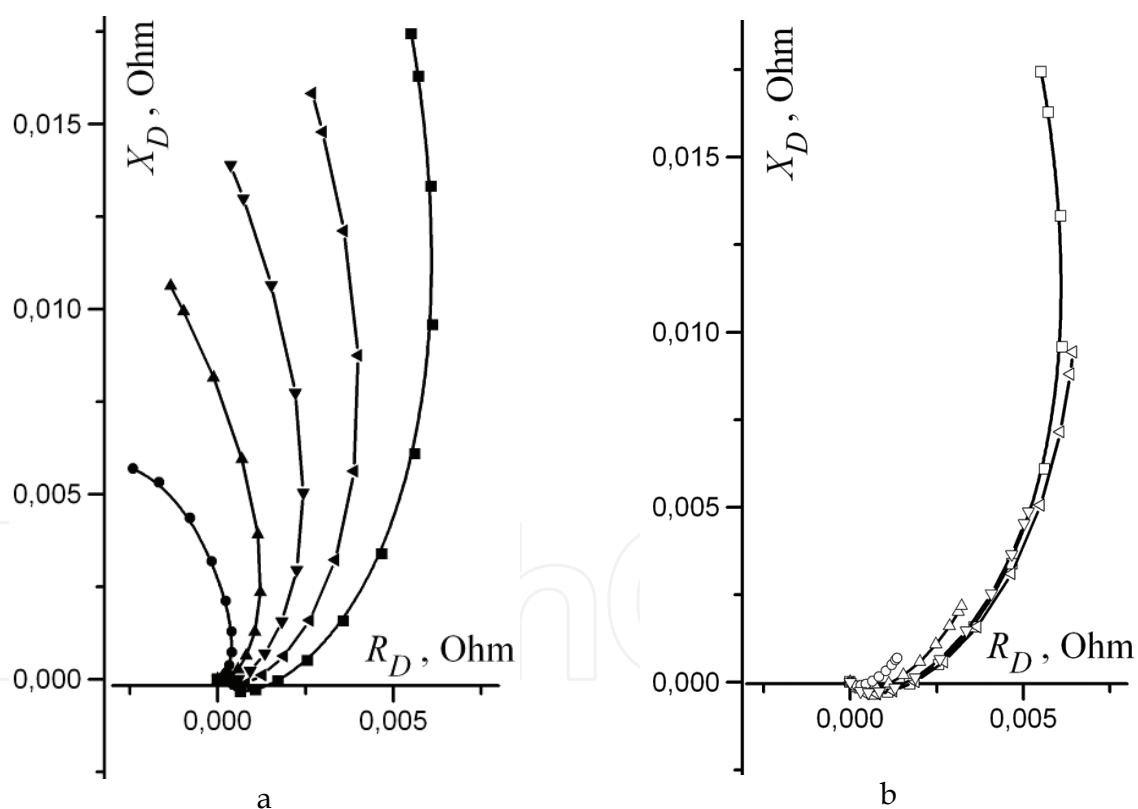


Fig. 10. EC probe scanning hodographs for holes situated on internal (a) and external (b) tube surfaces for hole depth 0.3 mm (• and ○); 0.6 mm (▲ and Δ); 0.9 mm (▼ and ▽); 1.2 mm (◄ and ►) and 1.5 mm (■ and □).

It can be noticed, that depth of the hole for internal and external defects influences the hodographs pattern. For any tube surface the defect depth growth lead to amplitude growth and the hodograph rotation. The amplitude changes for subsurface defects on external tube

surface are more considerable than amplitude changes for surface defect on internal tube surface. It seems that the hodograph rotation and phase changes are stronger for surface defects in comparison with such changes for defects on external tube surface. Such feeling is wrong and this statement was confirmed, when more scrupulous analyze was done. When depth of surface defect is increased from 0.3 mm to 1.5 mm, the phase of signal response in the points of amplitude maximum is changed on 32.4° from 104.8° to 72.4° (Fig. 10a). The same growth of the depth for subsurface defect rotate the hodographs in counterclockwise direction and phase is changed on 45° from 26.9° to 72.4° (Fig. 10b). This conclusion is confirmed by next diagrams (Fig. 11), whereon the amplitude and phase in the points of EC probe maximum amplitudes in dependence versus the defect depth independently of the tube surface the defects were originated are presented. Black marks correspond with the surface defects on the internal tube surface and the white marks are fitted with defects on outer tube surface.

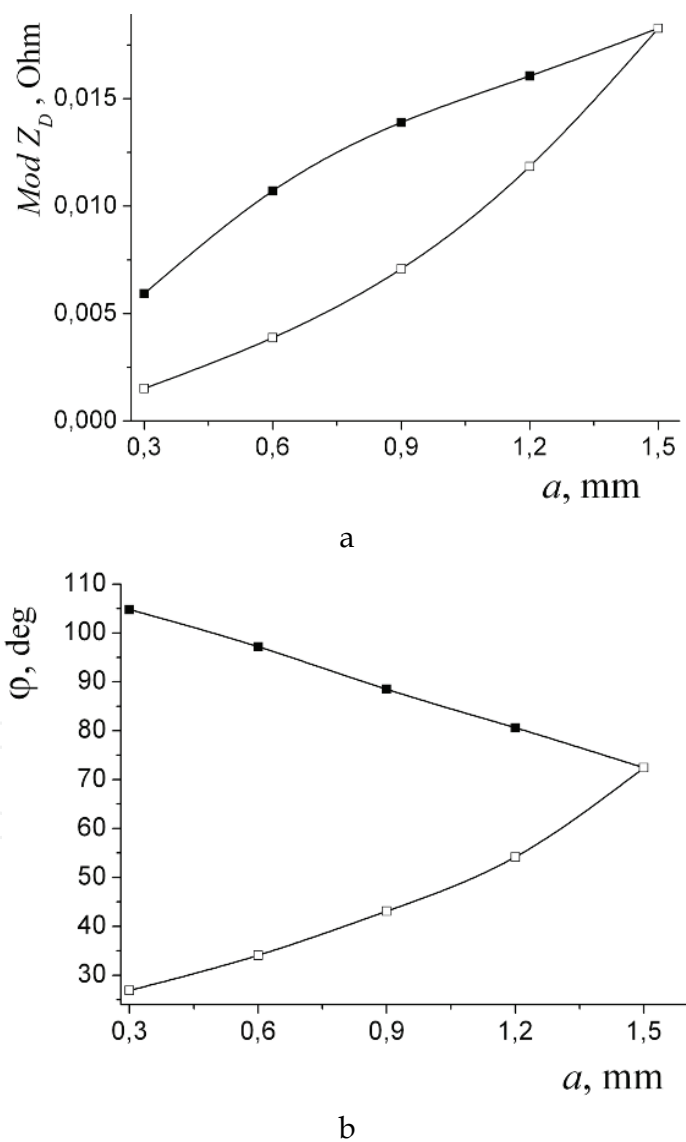


Fig. 11. Influence of defect depth  $a$  on the EC probe signal response amplitude (a) and phase (b) for holes situated on internal ( $\blacksquare$ ) and external ( $\square$ ) tube surfaces.

Depth-amplitude diagram on Fig. 11a show, that the same amplitude can be corresponded with two different defects, situated on different tube surfaces. Thereby, the signal amplitude doesn't give the possibility for recognition of defects situated on different tube surfaces. Such recognition can be obtained by phase measurements. The depth-phase diagrams similar to presented on Fig. 11b are widely used in practice for defect depth estimations. It is important to notice, that such diagrams must to be obtained for specified EC probe, selected operational frequency and tube material. Very often this requirement is violated in practice, because of the difficulties in producing the reference standard set with different size defects needed for precise eddy current inspection equipment calibration.

### **3.2 The development of bobbin probe with enhanced breakage resistance and tube passing ability**

Unfortunately, low passing ability is the characteristic feature of tubes mounted in overwhelming majority of WWER type NPP. This circumstance is the root cause of considerable reduction of quantity of tubes, inspected by one bobbin probe, due rapid wear and cable breakage. To improve the bobbin probe breakage resistance and passing ability some new technical judgment were proposed (Mozhuchin et al., 2002; Najda et al., 2002).

Conventional bobbin probes for SG tube inspection consist of eddy current coils and long cables (such long as tube length) for connection with eddy current device. All cables are protected by tubular flexible sheath. Probes are moved along the tube by special push-puller system. During in-service life these cables are repeatedly wound on special drum for probes carrying purposes. For electronic noise suppression cables are executed to be coaxial. The weak point of conventional EC probe is the point of the connection of coil wires to the cable. Therefore the coil wires lost contact with cable during the windings on the drum. To prevent the probe damage the internal wires and cables must be longer than the tubular sheath. In conventional probes this difference is insufficient even when wires are produced to have wave like form (see for example Amedro et al., 1983). So, these probes have low operational reliability and resource, because the inspection technology provides multiple "winding - unwinding" cycles, when the inspected tubes are changed. The average lifetime of these probes is limited by 300 - 400 tube inspections. Despite the high price all damaged probes are throwing away because are not repairable due radionuclide contamination.

One of proposed probe (Najda et al., 2002) has inspection head 1 with EC coils and electrical connector 2, which are mounted on opposite sides of flexible tubular sheath 3 (Fig. 12). Tubular sheath can be executed in cylindrical helix form 4. Probe coils 5 are electrically connected to connector 2 by the cables 5 located inside the tubular sheath 3. The cables 5 are executed in the form of at least one pair of essentially straight sections, which alternate with sections, where cables have the form of cylindrical spiral springs with the adjacent turns in initial part. Cables 6 and 7 may be closely wound around the common axis 8 and 9 forming a common helix diameter (Fig. 12b). In alternative embodiment cables 10 and 11 can be wound in spirals around parallel axes 12 and 13 (Fig. 12c). The spiral sections of one cable are shifted relatively the spiral sections of second cable to some distance 14 and situated near its rectilinear sections. The alternative embodiment of proposed invention with most compact version of cable laying is presented in Fig. 12d. Here straight sections of each cable are situated inside a cylindrical spiral springs areas of second cable.

In the initial state the tubular sheath 3 of EC probe is straightened and the spiral spring turns 6 and 7 are compressed and fitted each other. When tubular sheath is wound on the

drum the possible cable length deficit is compensated by the spiral springs stretching. So during the multiple “winding - unwinding” cycles the cables are not displaced relative to the tubular sheath and not damaged.

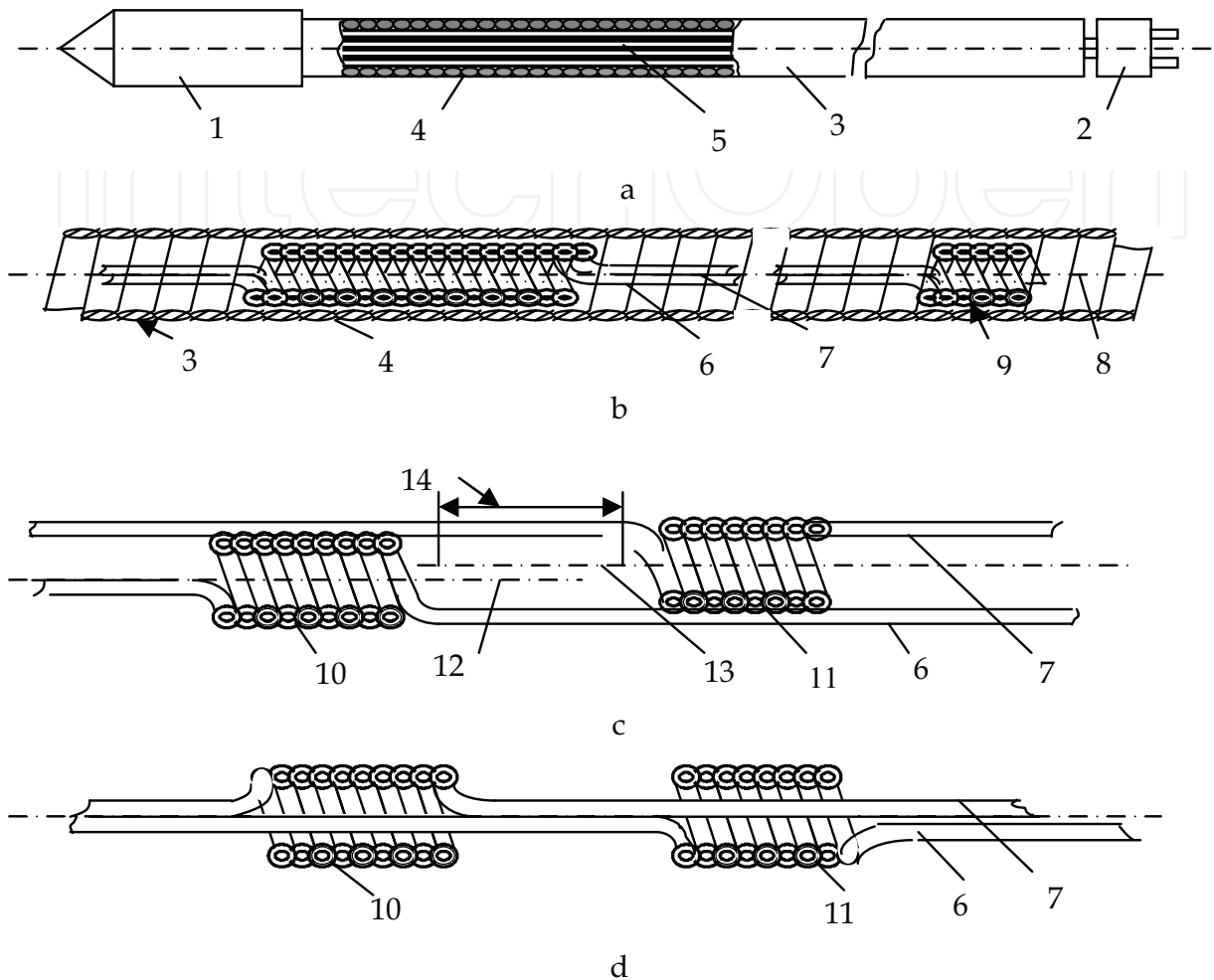


Fig. 12. Eddy current probe with improved resistance: a – general arrangement; b, c and d – alternative embodiments with different cable laying.

The next step in EC probe improvements was the increase the possibility to pass through bended zones of SG heat exchanger tubes. To solve this problem the new construction (Fig. 13) of EC probe was proposed (Mozhuchin et al., 2002). Improved EC probe is supplied by spiral 4 mounted to inspection head 1. Close to inspection head section 6 of spiral 4 is executed with clearance between spiral turns. The length of this section  $L$  is equal to  $2-15 d$ , where  $d$  – spiral diameter. The rest section of spiral 4 can be executed with contacting turns. Section 6 can be executed with changing cross-section area of spiral turns. In this case the spiral thickness monotonously increases from the head 1 toward the connector 2. In Fig. 13a and Fig. 13b alternative embodiments of presented improvement are presented. Spiral profile in section 6 can be produce to be constant in outer (Fig. 13a) or internal (Fig. 13b) spiral diameters. The embodiment on Fig. 13b is more technological. Thus, in all cases the part at the front end of the spiral section 6 is made with weakened bending resistance for better tube passing ability.



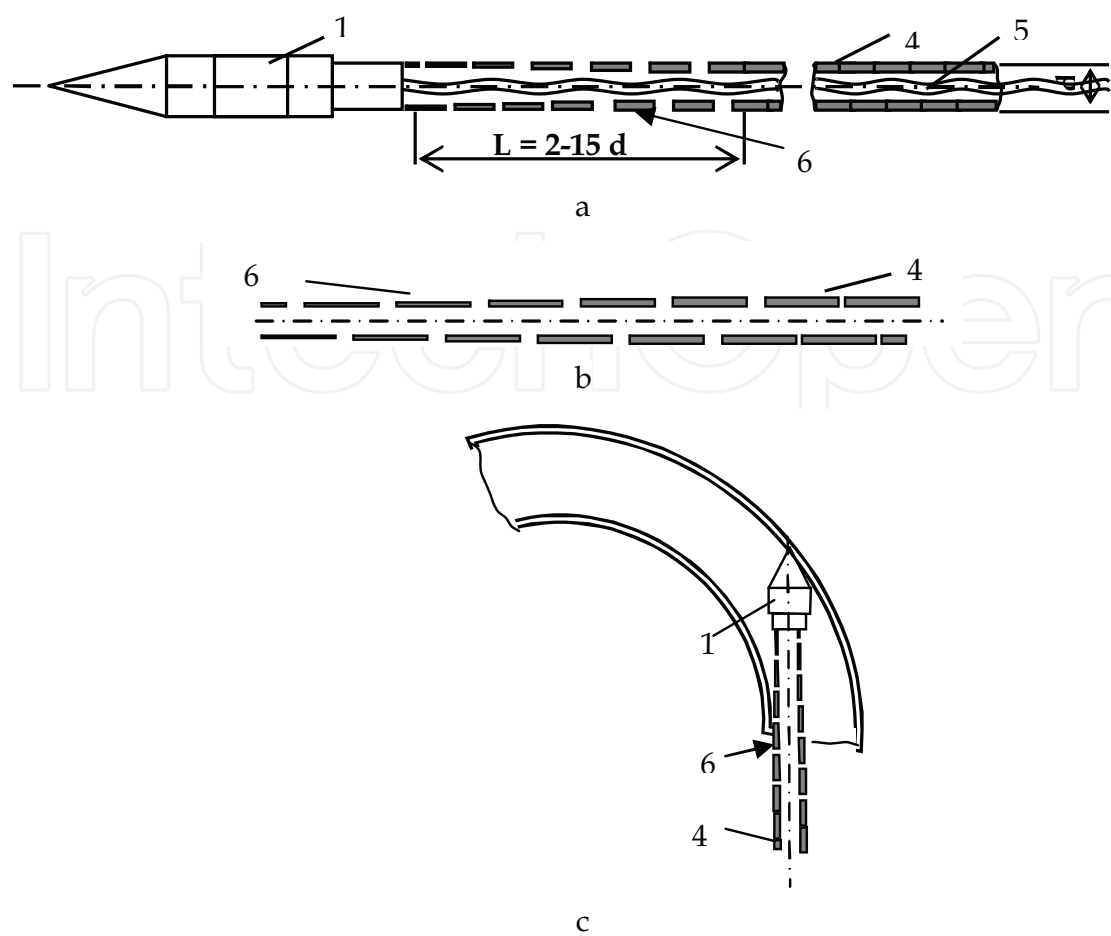


Fig. 13. Different embodiments of eddy current probe with improved passing ability (a, b) and eddy current probe in bended part of tube (c).



Fig. 14. EC probes for heat exchanger tube inspection.

The increased resistance and passing ability of improved EC probes (Fig. 14) was confirmed by in-service inspection of PGV type SG on Zaporizhia NPP. The quantity of tubes tested by one improved probe was increased more then 5 times in relation to conventional EC probes.



#### 4. The development of automated system for eddy current inspection of collector wall cracking.

The defect detection in NPP collector wall must be executed in conditions of high level of radiation and pollution. So, full automation of inspection operations it is assumed to be applied. In addition, for EC probe protection the protective cover, which reduce the EC probe sensitivity also it is needed. In addition the defect detection in collector wall can be executed only through the heat exchanger tube wall.

The block diagram of developed automated system for inspection of collectors is shown in Fig. 15. The system includes a manipulator, unit for servo drive controlling, TV positioning unit, remote operator working place, industrial computer and eddy current flow detector device with rotary scanner for superimposed EC probe rotation (Najda et al., 2008).

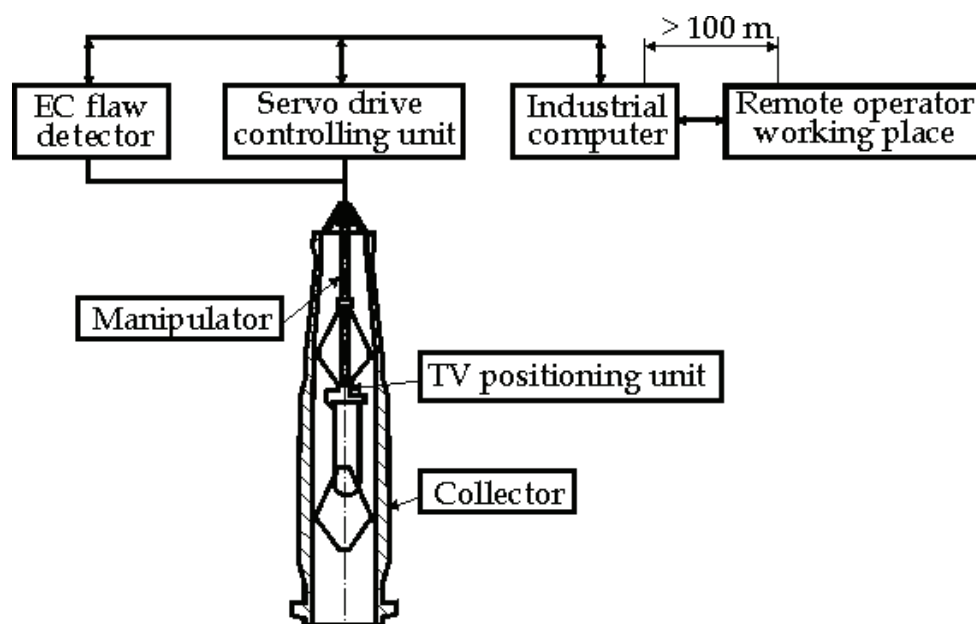


Fig. 15. The generalized scheme of the automated EC system for collector wall inspection.

As the inspection part of the automated EC system it is supposed to use the EC flaw detector Elotest N320 developed by Rohmann GmbH (Germany), which provides the necessary facilities needed for automated system creation, in particular:

- Remote control via Ethernet channel, which allows flaw device managing from remote computer;
- The ability to record and store device settings and obtained inspection signal responses needed for database creation;
- Representation of signal responses in X-Y, X-t, Y-t or C-Scan form, which provides advanced visual and programmed signal responses analysis;
- The possibility to realize the two-frequency signal processing and filtering by software mode application for better suppression of disturbing factors influence;
- Open data transfer protocol for creation of the software based on specific parameters of the inspected object.

The manipulator (Fig. 16a) is intended for EC probe displacement in the vertical, azimuthal and radial directions (Fig. 16b) for introduction to the collector inlet holes (Fig. 1a). The manipulator can be operated in automatic mode on defined inspection map and in manual

mode. A specific feature of the developed manipulator is a mechanism for coaxial connection of inspection head to inlet holes, which in the initial state have the deviation from concentricity and parallelism.

To scan the inner surface of tubes in the collector wall zone special rotary scanner was designed (Fig. 16c), which provides the tube internal surface scanning by helical trajectory with speed to 3000 rpm needed for dynamic mode of signal processing. In contrast to some other inspection systems, the developed scanner was supplied with the protective stainless steel cover to prevent the EC probe radioactive contamination.

The unit for servo drives controlling was intended to receive the commands from remote operator working place, to control the signal formation for manipulator and to transfer the information about the current servo drive parameters to operator working place.

Positioning unit is used to define the presence of plug in the inlet hole, as well as for centring of the inspection head with EC probe in inlet hole of inspected tube. The positioning unit operation is based on the processing of television images and the application of the pattern recognition algorithms. As a result of television information processing unit make a decision about the presence of plug in the heat exchanger tube, form a signal about possible displacement in the vertical and horizontal planes for servo drive controlling.

The automated operator working place is intended to manage the system, to organize the interaction of the operator interface with the system, to display and store the inspection results and to analyse the collector wall technical condition.

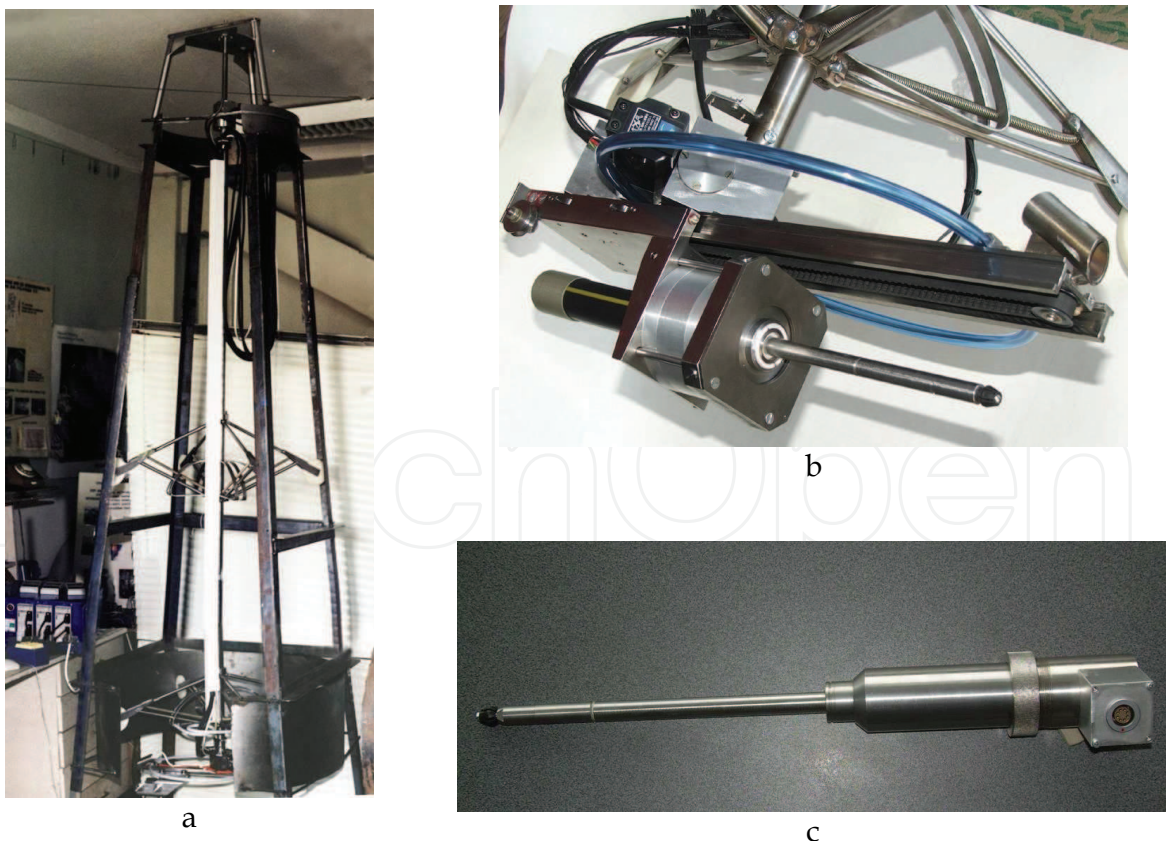


Fig. 16. The manipulator (a), mechanism for inspection head displacement (b) and rotary scanner with EC inspection head (c).

For better noise suppression the two-frequency mode for EC probe excitation (12 and 60 kHz) in combination with signal filtering in dynamic mode were applied. The defect signal response after amplification and processing can be presented in the complex plane in the form of the hodograph with characteristic amplitude (pick-to-pick distance) and phase (hodograph orientation). By the signal response amplitude and phase analysis the detected defects can be classified and defect parameters, in particular its depth, can be estimated. The sensitivity threshold for collector inspection is adjusted to be equivalent to artificial defect with depth 1.0 mm and width (opening) 0.3 mm. To simulate the defects with different depth two types of reference standards (Fig. 17) with artificial like crack defects were proposed (Najda et al., 2008; Uchanin et al., 2009).

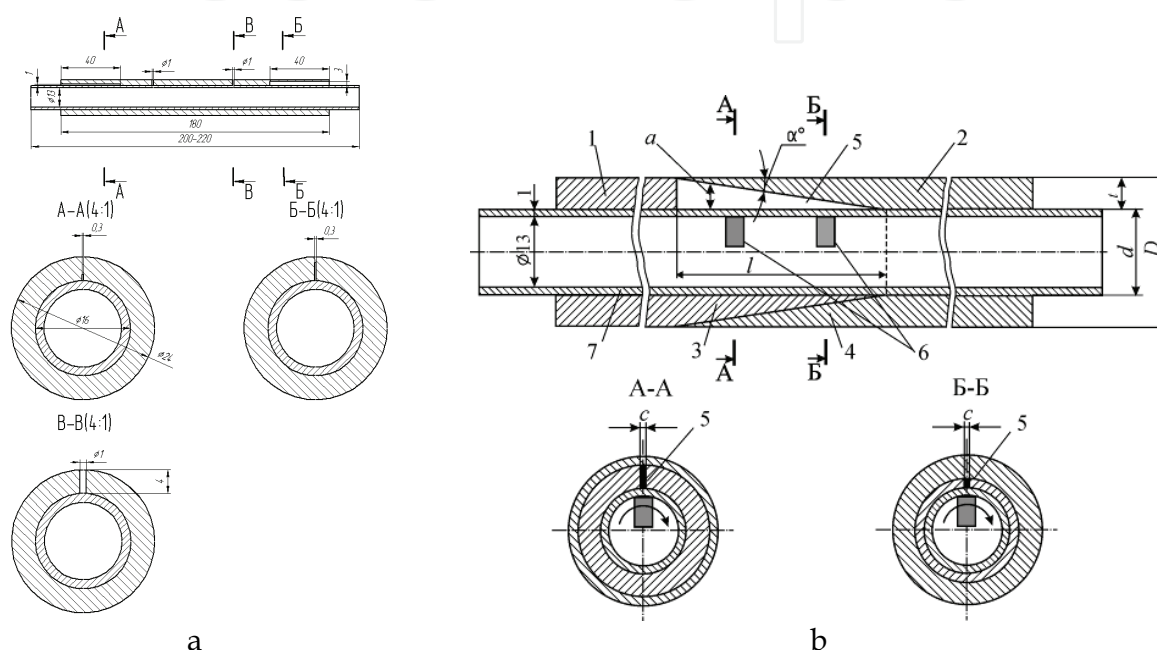


Fig. 17. Reference standard for 1 mm and 3 mm flaw depths simulation (a) and combined reference standard for different depth defects simulation in dynamical mode.

Reference standard on Fig. 17a is easier in producing, but can simulate cracks with 1 mm and 3 mm depth only. Combined reference standard (Fig. 17b) can be applied only in dynamic mode, when EC probe signal response from conical junction of two parts 1, 2 with length  $l$  during EC probe 6 rotation is suppressed. Crack signal response is simulated by longitudinal cut 5 in conical part 1. The defect depth can be chosen by change of EC probe location.

To detect the cracks in collector wall throw the tube wall and the protective cover special superimposed small size multidifferential type EC probes (specified as Leotest MDF) were developed in Leotest-Medium Center (Lviv, Ukraine). This type EC probes were investigated in many known European scientific organizations, such as Otto-von-Guericke University (Magdeburg), Fraunhofer Institute for non-destructive testing (Saarbrücken), Kontroll Technik GmbH (Schwarmstedt) at alias (Uchanin et al., 2002; Uchanin, 2006; Uchanin et al., 2006; Mook et al., 2007; Uchanin, 2009). The main task for developed EC probe is to detect 1.0 mm depth defect throw 1.5 mm tube wall thickness plus 1 mm protective cover thickness. The signal response for 1 mm depth defect in complex plane on EC device screen is presented on Fig. 18.

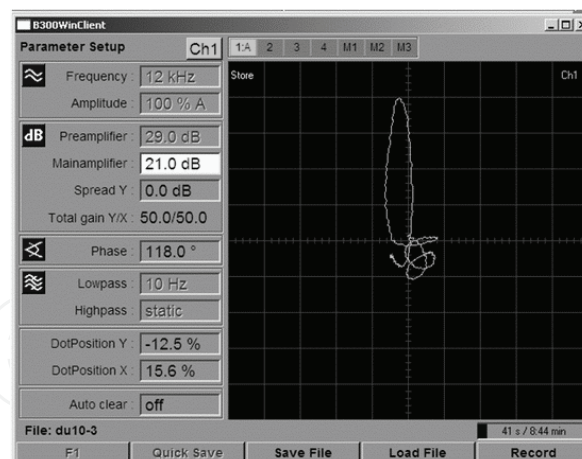


Fig. 18. Complex plane signal response obtained for 1 mm depth defect in reference standard (Fig. 17a).

Presented signal responses (Fig. 18) confirm good sensitivity and low noise level of developed EC system, when defect detection is performed through the heat exchanger tube wall.

## 5. Conclusion

In this chapter the results of bobbin type EC probe signal response investigation are presented. The specific features of signal response distribution for cracks of different orientation, length and depth are analyzed. The inspection procedure for defect parameters estimation is discussed. The results obtained were used for bobbin type EC probe optimization and can be applied for inspection data interpretation.

The results of new EC bobbin probes development also are presented. For better tube passing ability special structural arrangements of EC probe constructions were proposed. It is especially important for examination of WWER type SG tubes because of inconvenient geometry and/or clogging.

The automatic EC system for detection of cracks in collector wall with rotary low frequency superimposed EC probe is presented. The developed automatic system consists of rotary scanner with EC head, EC flaw detector device, manipulator supplied with TV positioning unit for controlling the inspection head introduction to inlet holes, industrial computer for tested data collection and remote operator working place. The performance of developed low frequency superimposed EC probe confirms good sensitivity of developed EC system.

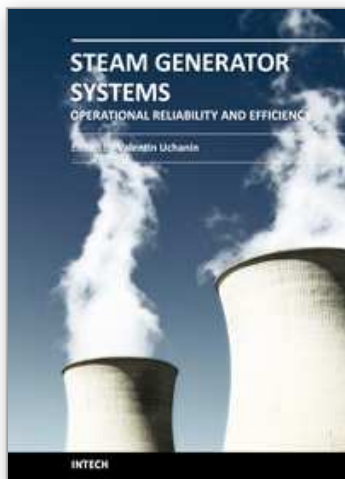
## 6. References

- Alferink, R. & Meier, J. (1996). Detection and quantification of axial crack in heat exchanger tubes. *Insight*, Vol. 38, No 10, pp. 711-714. ISSN 1354-2575.
- Amedro, A., Audemard, B. & De Mull, R. (1983). Eddy current inspection probe for non-destructive inspection of tubes with a probe body having an outer coiled spring sheath and an inner plastic material sheath. US patent № 4413231, G01N27/72.
- Balitskii, A., Makhnenko, O., Balitskii, O., Grabovskii, V., Zaverbnyi, D. & Timofeev, B. (2005). *Strength of Materials and Durability of Structural Elements of Nuclear Power*



- Plant: Handbook* (in Ukrainian), Vol. 8, Akadempriodika, ISBN: 966-360-035-7, Kyiv, Ukraine.
- Bisiaux, B., Pichenot, G., Prémel, D., Reboud, C. & Lesselier, D. (2006). Simulation of 3D Eddy Current testing of Tubes with external Probes: Modeling Approach and Experimental Validations, *Proceedings of 9-th Europ. Conf. on NDT*. [www.ndt.net](http://www.ndt.net). Paper We.2.3.1. Berlin, Germany.
- Cecco, V., Sharp, F. & Marini, L. (1996). Differential transmit-receive eddy current probe incorporating bracelets of multi-coil units. US patent № 5506503, G01N27/90.
- Clark, W. (1993). Multiple-element eddy current probes for enhanced inspection. *Materials Evaluation*, № 6, pp. 794-802, ISSN: 0025-3327.
- Dunbar, W.S. (1985). The Volume Integral Method of Eddy Current Modeling. *J. Nondestructive Evaluation*, Vol. 5, № 1, pp. 9-14, ISSN: 0195-9298.
- Herka, M.; Kubis, S., Ilencik, K. & Krajcovic, R. (1999). Degradation monitoring of steam generator tubes of VVER 440 NPP using eddy current technique, *Proceedings of Joint EC-IDEA Meeting "NDT Methods for Monitoring Degradation"*. pp. 215-220, Petten, Netherlands.
- Hofler, J. (1999). Additional Steam Generator Eddy Current Inspection Techniques, *Proceedings of Joint EC-IDEA Meeting "NDT Methods for Monitoring Degradation"*. pp. 31-37, Petten, Netherlands.
- IAEA-TECDOC-981. (1997). Assessment and management of ageing of major nuclear power plant components important to safety: Steam generators. International atomic energy agency. Vienna, Austria, 173 p.
- IAEA-EBP-WWER-11. (1998). Methodology for qualification of in-service inspection systems for WWER nuclear power plants. International atomic energy agency. Vienna, Austria, 21 p.
- IAEA-TECDOC-1400. (2004). Improvement of in-service inspection in nuclear power plants. International atomic energy agency. Vienna, Austria, 38 p.
- Ida, N. (1986). Computer modeling of eddy current field, In: *Nondestructive testing handbook*, 2nd ed. by R. McMaster & P. McIntire, Vol. 4, pp. 561-590, American Society for Nondestructive Testing, ISBN: 0-931403-01-4, USA.
- Krajcovic, R. & Plasek, J. (2006). Eddy Current Inspection of WWER Steam Generator Tubes – Sensitivity of Bobbin Probe Technique. *Proceedings of 9-th Europ. Conf. on NDT* ([www.ndt.net](http://www.ndt.net)). - Index Th.3.1.4. Berlin, Germany.
- Laube, U., Grigoriev, M. & Lovchev, V. (2006). In-service Inspection of Russian VVER Nuclear Power Plants, *Proceedings of 9-th Europ. Conf. on NDT*. ([www.ndt.net](http://www.ndt.net)). Paper P166. Berlin, Germany.
- Melechov, R. & Pochmurskij, V. (2003). *Constructional materials of power equipment* (in Ukrainian), Naukova dumka, ISBN: 966-00-0150-9, Kyiv, Ukraine
- Mook, G., Hesse, J. & Uchanin, V. (2007). Deep Penetrating Eddy Currents and Probes. *Materials Testing*, Vol. 49, №5. pp. 258-264.
- Mozhuchin, A., Kovbasenko, O., Pyshnyj, V., Lobanov, O. & Najda, V. (2002). The probe for inspection of long curved tubes (in Ukrainian). Ukrainian patent № 50074, G01N27/90.
- Mytrofanov, A.; Neklyudov, I. & Ozhygov, L. (2008). In-service defects in the heat exchanger tubes of steam generators at nuclear power plants. *Material Science*, Vol. 44, No. 4, pp. 589-593, ISSN: 1068-820X.

- Najda, V., Pyshnyj, V., Moszhuchin, A., Kovbasenko, O., Chizhenko, V. & Lobanov, O. (2002). The probe for non-destructive inspection of tube metal state and method for of its realization (in Ukrainian). Ukrainian patent № 50073, G01N27/90.
- Najda, V., Uchanin, V., Moszhuchin, A., Gogulia, O. & Gulko, V. (2008). The development of system for automated eddy current inspection of nuclear power plants collectors (in Russian). *Technical diagnostic and nondestructive testing*, No. 3, pp. 21–24, ISSN: 0235-3474.
- Nam Jo. & Hyang-Beom Lee. (2009). A novel feature extraction for eddy current testing of steam generator tubes. *NDT&E International*, Vol. 42, pp. 658-663, ISSN: 0963-8695.
- Neklyudov, I., Azhazha, V., Ozhygov, L., Mytrofanov, A.; Krajniuk, Je. & Lisna, V. (2006). Atlas of the operational defects in steam generator heat exchanger tubes of power units of NPP with VVER type reactors (in Ukrainian), In: *The problems of life-time and safty of constructions, buildings and machines*, Ed. B. Paton, pp. 157-160, Paton electric welding institute, ISBN 966-8872-04-5, Kyiv.
- Pichenot, G., Buvat, F., Maillot, V. & Voillaume, H. (2004). Eddy Current Modelling for Nondestructive Testing. *Proceedings of 16 World Conf. for NDT* (www.ndt.net). Montreal, Canada.
- Sabbagh, H., Murphy, R., Sabbagh, E. & Alrin, J. (2008). Application of model based inversion to eddy current NDT of heat exchanger tubing. *Materials Evaluation*, № 7, pp. 764-774, ISSN: 0025-3327.
- Song, S., Kim, Y., Kim, E. & Choi, Y. (2003). Model-based interpretation of experimental eddy current signals obtained from steam generator tubes by bobin probe. *Insight*, Vol. 45, No 5, pp. 337-343, ISSN 1354-2575.
- Uchanin, V., Mook, G. & Stepinski, T. (2002). The investigation of deep penetrating high resolution EC probes for subsurface flaw detection and sizing. *Proceedings of the 8 European Conf. on NDT* (www.ndt.net). Barselona.
- Uchanin, V. (2006). Eddy current multidifferential probes and their application (in Russian). *Technical diagnostic and nondestructive testing*, No. 3, pp. 34–41, ISSN: 0235-3474.
- Uchanin, V., Lutcenko, G. & Nikonenko, A. (2006). Automated Eddy Current System for Flaw Detection and Sizing during In-service Stainless Steel Tube Inspection, *Proceedings of 9 European Conf. on NDT*. (www.ndt.net). Berlin.
- Uchanin, V. (2009). Analysis of the signals of the internal coaxial eddy current converter for flaw of pipes of steam generators. *Material Science*, Vol. 45, No. 3, pp. 448–452, ISSN: 1068-820X.
- Uchanin, V., Najda, V., Kirichenko, I. & Gogulia, J. (2009). The reference standard for adjustment, calibration and certification of eddy current flaw detectors (in Ukrainian). Ukrainian patent № 2008 10692, G01N27/90.
- Werner, R., Bernus, L. & Jacob, H. (1987). Development of multi-channel eddy current examination system for automated inspection of steam generator tubing, *Proceedings of Europ. Conf. on NDT*. Vol. 4, pp. 2572-2580. London.
- Wong, B., & Tan, K. (1995). Softwere developed to analyse the signals from the eddy current inspection of heat exchanger tubes. *Insight*, Vol. 37, No 2, pp. 87-92, ISSN:1354-2575.



## **Steam Generator Systems: Operational Reliability and Efficiency**

Edited by Dr. Valentin Uchanin

ISBN 978-953-307-303-3

Hard cover, 424 pages

**Publisher** InTech

**Published online** 16, March, 2011

**Published in print edition** March, 2011

The book is intended for practical engineers, researchers, students and other people dealing with the reviewed problems. We hope that the presented book will be beneficial to all readers and initiate further inquiry and development with aspiration for better future. The authors from different countries all over the world (Germany, France, Italy, Japan, Slovenia, Indonesia, Belgium, Romania, Lithuania, Russia, Spain, Sweden, Korea and Ukraine) prepared chapters for this book. Such a broad geography indicates a high significance of considered subjects.

### **How to reference**

In order to correctly reference this scholarly work, feel free to copy and paste the following:

Valentin Uchanin and Vladimir Najda (2011). The Development of Eddy Current Technique for WWER Steam Generators Inspection, Steam Generator Systems: Operational Reliability and Efficiency, Dr. Valentin Uchanin (Ed.), ISBN: 978-953-307-303-3, InTech, Available from: <http://www.intechopen.com/books/steam-generator-systems-operational-reliability-and-efficiency/the-development-of-eddy-current-technique-for-wwer-steam-generators-inspection>

**INTECH**  
open science | open minds

### **InTech Europe**

University Campus STeP Ri  
Slavka Krautzeka 83/A  
51000 Rijeka, Croatia  
Phone: +385 (51) 770 447  
Fax: +385 (51) 686 166  
[www.intechopen.com](http://www.intechopen.com)

### **InTech China**

Unit 405, Office Block, Hotel Equatorial Shanghai  
No.65, Yan An Road (West), Shanghai, 200040, China  
中国上海市延安西路65号上海国际贵都大饭店办公楼405单元  
Phone: +86-21-62489820  
Fax: +86-21-62489821



© 2011 The Author(s). Licensee IntechOpen. This chapter is distributed under the terms of the [Creative Commons Attribution-NonCommercial-ShareAlike-3.0 License](https://creativecommons.org/licenses/by-nc-sa/3.0/), which permits use, distribution and reproduction for non-commercial purposes, provided the original is properly cited and derivative works building on this content are distributed under the same license.

IntechOpen

IntechOpen